*Journal of Statistical Physics, Vol. 112, Nos. 3/4, August 2003 (© 2003)*

# Extension of the Lattice-Boltzmann Method for Direct Simulation of Suspended Particles Near Contact

**E-Jiang Ding[1] and Cyrus K. Aidun[2]**

*Received December 4, 2001; accepted February 14, 2003*

Computational methods based on the solution of the lattice-Boltzmann equation have been demonstrated to be effective for modeling a variety of fluid flow systems including direct simulation of particles suspended in fluid. Applications to suspended particles, however, have been limited to cases where the gap width between solid particles is much larger than the size of the lattice unit. The present extension of the method removes this limitation and improves the accuracy of the results even when two solid surfaces are near contact. With this extension, the forces on two moving solid particles, suspended in a fluid and almost in contact with each other, are calculated. Results are compared with classical lubrication theory. The accuracy and robustness of this computational method are demonstrated with several test problems.

**KEY WORDS:** Particle-particle and particle-wall interaction; lubrication force between surfaces near contact.

## 1. INTRODUCTION

It is well known that transport of solid particles suspended in fluid occurs in many physical and industrial processes. To analyze and understand the transport of suspensions, the motion and dynamics of solid particles suspended in fluid must be thoroughly studied. In the direct simulation of suspensions using continuum models of two-phase flows, the fluid dynamics is governed by the Navier–Stokes equations while the motion of the solid particles is governed by the Newtonian dynamics equation. An alternative method to continuum mechanics is the solution of the lattice-Boltzmann equation for the fluid phase. This is a robust and efficient

[1] Institute of Paper Science and Technology at Georgia Institute of Technology, 500 10th Street, N.W., Atlanta, Georgia 30318.

[2] Woodruff School of Mechanical Engineering, Georgia Institute of Technology, 801 First Drive, N.W., Atlanta, Georgia 30332-0405.



0022-4715/03/0800-0685/0 © 2003 Plenum Publishing Corporation

computational method for the analysis of solid particles suspended in fluid.[1–9] By combining Newtonian dynamics of the solid particles with a lattice-Boltzmann model of the fluid, the motion of the suspended particles can be simulated efficiently and accurately. An obvious advantage of the lattice-Boltzmann (LB) method is that the computer code can be easily implemented on parallel processors because of the local nature of the time evolution operator. Another advantage of this method is that the computational time is independent of the Reynolds number and weakly dependent on the number of solid particles, although it is dependent on the size of the computational domain. The present work is on the improvement of the computational method for cases where two particles come to near contact.

The lattice-Boltzmann method is first applied to suspended particles by Ladd.[1, 2] The algorithm constructed in Ladd's model is flexible and efficient. It requires fluid to cross the boundary of the suspended solid particle and occupy the entire domain. The solid-fluid boundary condition introduced in this method is momentum conserved as long as the momentum of the fluid inside and outside the solid particle are included. This method is applied to spherical surfaces in close contact by including the leading order lubrication force where the separation distance is closer than about a lattice space.[10, 11] The limitation of this version of the LB method is that it can only be used for solid particles with density larger than the fluid density.

In an alternative approach by Aidun *et al.*,[3, 4, 6] the fluid interior to the solid particle is eliminated and the method is extended to any solid-to-fluid density ratio. However, as in any discrete computational method, the LB method in general is limited to the gap width between solid particles larger than the size of the lattice unit. As the solid particles get too close to each other, leaving no fluid node between the solid surfaces, the LB method does not accurately calculate the hydrodynamic interaction between the solid particles. In order to resolve the hydrodynamic force between solid particles near contact, relatively large numbers of lattice nodes need to be used in the computational domain. One approach to resolve this difficulty is to amend the solid-fluid interaction calculation with a model of lubrication force based on theoretical lubrication approximation[10, 11] for a small gap between regular shaped objects. In Section 2.6 we discuss a local link-by-link implementation of the lubrication force when the gap between particles becomes very small.

With the method by Aidun, Lu, and Ding (ALD),[6] as long as there are at least two fluid lattice nodes in between solid surfaces near contact, the hydrodynamic forces are computed correctly. In order to remove this restriction and resolve the hydrodynamic interaction between particles without the requirement of two or more lattice nodes in between the solid

surfaces, "virtual nodes" are added to the solid boundaries. The only influence of the virtual boundary nodes is to provide the means to calculate the hydrodynamic forces, even when the separation between solid surfaces is less than a lattice unit. By this simple amendment of the ALD method, the ALD' method is able to correctly calculate the interaction between solid objects near contact. The accuracy of the simulation can be greatly improved even though the computational domain consists of fewer lattice nodes.

The remaining part of this paper is organized as follows. The ALD' method is outlined in Section 2. It is demonstrated in Section 3 that this method is robust with no adjustable parameters. In Section 4, the lubrication force for several different cases is computed with the ALD' method and the results are compared with lubrication theory demonstrating the reliability of the present extension. Some concluding remarks are included in Section 5.

## 2. THE ALD' METHOD

### 2.1. Lattice-Boltzmann Equation

The state of the fluid at node $\mathbf{x}$ at time $t$ is described by the distribution function $f_{\sigma i}(\mathbf{x}, t)$, which is calculated through the lattice-Boltzmann equation:[12–15]

$$f_{\sigma i}(\mathbf{x}+\mathbf{e}_{\sigma i}, t+1) = f_{\sigma i}(\mathbf{x}, t) - \frac{1}{\tau}[f_{\sigma i}(\mathbf{x}, t) - f^{(0)}_{\sigma i}(\mathbf{x}, t)], \tag{1}$$

where $\tau$ is the relaxation scale and $\mathbf{e}_{\sigma i}$ is the velocity vector, pointing from node $\mathbf{x}$ to the adjacent nodes in a square or cubic lattice structure for two-dimensional or three-dimensional cases, respectively. The magnitude of $\mathbf{e}_{\sigma i}$ is determined by the first subscript, $\sigma$, for the resting particles

$$|\mathbf{e}_{0i}| = c_0 = 0, \qquad i = 1,$$

for particles moving to off-diagonal nodes,

$$|\mathbf{e}_{1i}| = c_1 = 1, \qquad \begin{cases} i = 1,\ldots, 6 \text{ in three-dimension and} \\ i = 1,\ldots, 4 \text{ in two-dimension,} \end{cases}$$

and for particles moving to the diagonal nodes,

$$|\mathbf{e}_{2i}| = c_2 = \sqrt{2}, \qquad \begin{cases} i = 1,\ldots, 12 \text{ in three-dimension and} \\ i = 1,\ldots, 4 \text{ in two-dimension.} \end{cases}$$

$f_{\sigma i}^{(0)}(\mathbf{x}, t)$ is the equilibrium distribution function, defined as

$$f_{\sigma i}^{(0)}(\mathbf{x}, t) = \rho(\mathbf{x})[A_\sigma + B_\sigma(\mathbf{e}_{\sigma i} \cdot \mathbf{u}) + C_\sigma(\mathbf{e}_{\sigma i} \cdot \mathbf{u})^2 + D_\sigma u^2], \tag{2}$$

where the density $\rho$ and the continuum velocity vector $\mathbf{u}$ of the fluid are defined as

$$\rho(\mathbf{x}, t) = \sum_{\sigma, i} f_{\sigma i}(\mathbf{x}, t) \qquad \text{and} \qquad \mathbf{u}(\mathbf{x}, t) = \frac{1}{\rho(\mathbf{x}, t)} \sum_{\sigma, i} f_{\sigma i}(\mathbf{x}, t)\, \mathbf{e}_{\sigma i},$$

respectively.

The probability distribution function, $f_{\sigma i}(\mathbf{x}, t)$, updated by

$$f_{\sigma i}(\mathbf{x}, t+1) = \mathsf{P}_0 \mathsf{C} f_{\sigma i}(\mathbf{x}, t), \tag{3}$$

where the propagator, $\mathsf{P}_0$, and the collision operator, $\mathsf{C}$, are defined as

$$\mathsf{P}_0 f_{\sigma i}(\mathbf{x}, t_+) \equiv f_{\sigma i}(\mathbf{x} + \mathbf{e}_{\sigma i'}, t_+) \tag{4}$$

and

$$f_{\sigma i}(\mathbf{x}, t_+) = \mathsf{C} f_{\sigma i}(\mathbf{x}, t) \equiv f_{\sigma i}(\mathbf{x}, t) - \frac{1}{\tau}[f_{\sigma i}(\mathbf{x}, t) - f_{\sigma i}^{(0)}(\mathbf{x}, t)], \tag{5}$$

respectively. Here, $(\sigma i')$ always means the link with direction opposite to that of link $(\sigma i)$, and $t_+$ is the time immediately after the collision, that is $t_+ - t \ll 1$ (recall the time step is set to unity). One step of lattice-Boltzmann simulation is then divided into two successive operators. The results of the collision operator are dependent on the choice of the equilibrium distribution function, which will be discussed in Section 2.2. The propagator will change its form, depending on the boundary condition, which will be considered in Section 2.4.

## 2.2. The Equilibrium Distribution Function

The coefficients in the equilibrium distribution functions are determined by conservation laws for mass, momentum, and kinetic energy. These constrains in two-dimensional cases have turned out to be:[4, 14]

$$\begin{array}{llll} & B_0 = 0, & C_0 = 0, & \\ A_1 = \frac{1}{2}(1 - A_0 - c_s^2), & B_1 = \frac{1}{3}, & C_1 = \frac{1}{2}, & D_1 = -\frac{1}{2}(1 + D_0), \\ A_2 = -\frac{1}{4}(1 - A_0 - 2c_s^2), & B_2 = \frac{1}{12}, & C_2 = \frac{1}{8}, & D_2 = \frac{1}{8}(1 + 2D_0). \end{array} \tag{6}$$

The simplest expressions (with a total of three zero coefficients) for the 9-bit equilibrium distribution function are obtained when $c_s^2 = 1/3$, $D_0 = 0$, and $A_0 = 1/2$:

$$\begin{aligned} A_0 &= \tfrac{1}{2}, & B_0 &= 0, & C_0 &= 0, & D_0 &= 0, \\ A_1 &= \tfrac{1}{12}, & B_1 &= \tfrac{1}{3}, & C_1 &= \tfrac{1}{2}, & D_1 &= -\tfrac{1}{2}, \\ A_2 &= \tfrac{1}{24}, & B_2 &= \tfrac{1}{12}, & C_2 &= \tfrac{1}{8}, & D_2 &= \tfrac{1}{8}. \end{aligned} \tag{7}$$

Other choices are also possible. Since

$$\frac{B_1}{B_2} = \frac{C_1}{C_2} = \frac{1}{4}$$

these coefficients can be determined by requiring

$$\frac{A_1}{A_2} = \frac{D_1}{D_2} = \frac{1}{4},$$

which gives the following coefficients:[14]

$$\begin{aligned} A_0 &= \tfrac{4}{9}, & B_0 &= 0, & C_0 &= 0, & D_0 &= -\tfrac{2}{3}, \\ A_1 &= \tfrac{1}{9}, & B_1 &= \tfrac{1}{3}, & C_1 &= \tfrac{1}{2}, & D_1 &= -\tfrac{1}{6}, \\ A_2 &= \tfrac{1}{36}, & B_2 &= \tfrac{1}{12}, & C_2 &= \tfrac{1}{8}, & D_2 &= -\tfrac{1}{24}. \end{aligned} \tag{8}$$

This set of coefficients will be used in this paper, because it is in agreement with the Boltzmann–Maxwell distribution function up to the order of $u^2$.[16]

In three-dimensional cases, the following coefficients will be used in this paper:

$$\begin{aligned} A_0 &= \tfrac{1}{3}, & B_0 &= 0, & C_0 &= 0, & D_0 &= -\tfrac{1}{2}, \\ A_1 &= \tfrac{1}{18}, & B_1 &= \tfrac{1}{6}, & C_1 &= \tfrac{1}{4}, & D_1 &= -\tfrac{1}{12}, \\ A_2 &= \tfrac{1}{36}, & B_2 &= \tfrac{1}{12}, & C_2 &= \tfrac{1}{8}, & D_2 &= -\tfrac{1}{24}. \end{aligned} \tag{9}$$

When the scaling for time, length, and, consequently, velocity, are all set to unity, the "kinematic viscosity" is given by $\nu = (2\tau - 1)/6$.[12] The relation between the "kinematic viscosity" in the lattice scale and the physical fluid viscosity is explained in Section 3. The Mach number, $M_a$, is given by the characteristic velocity defined in the lattice scale divided by $c_s$. In all cases, the characteristic velocity in the lattice scale is kept less than 0.1, giving a Mach number less than 0.173. As long as the velocity in the

lattice scale is small enough, the compressible characteristic of the fluid flow in the lattice scale is insignificant, and the method accurately simulates incompressible flow in the continuum scale.

## 2.3. Real and Virtual Nodes

As indicated before, in the early applications of lattice-Boltzmann to suspensions,[1, 2, 10, 11] fluid is required to occupy the entire domain, including the solid particles. In that approach, the fluid inside and outside the solid particle is physical fluid, that is, the total force and the total torque on the solid particle are contributed not only by the fluid nodes outside the solid particle but also the fluid nodes inside the solid particle. The particles comprise a solid shell of given mass and inertia, filled with fluid of the same mass density as the bulk fluid. As a result, the total mass density of the particle can never be less than the fluid density, limiting this approach to cases where the solid-to-fluid density ratio is greater than one.

In an alternative approach, with the ALD[3, 6] method, where solid particles are treated as real solid objects with no interior fluid nodes, the solid-to-fluid density ratio can be less than or greater than one. As the solid particles move, the fluid domain changes; some fluid nodes may be covered while new fluid nodes appear. The rules governing this process require additional steps which are not required in the Shell method. The advantages of both models can be combined by addition of "virtual nodes" inside the solid particle which contain "virtual fluid." The virtual fluid is characterized by having the same density as the real fluid. The nodes inside the solid particle and adjacent to the solid boundary are referred to as the "virtual boundary nodes." In contract to the Shell model, the nodes inside the solid particle have no influence on the mass and momentum transfer between the solid particle and the surrounding fluid. When fluid nodes completely surround the particle, the momentum from the physical fluid nodes is transferred to the solid particles, as in the ALD method. The components of the distribution functions at the virtual nodes are updated in every lattice-Boltzmann time step. The advantages of adding virtual boundary nodes will be explained in the following sections.

A small impulse of force is applied to the solid particle as a node is covered or uncovered. When a solid particle covers a physical node, the transferred force and torque are given, respectively, by

$$\mathbf{F}^{(c)}(\mathbf{x}, t_0 + \tfrac{1}{2}) = \rho(\mathbf{x}, t_0)[\mathbf{u}(\mathbf{x}, t_0) - \mathbf{U}'] \tag{10}$$

and

$$\mathbf{T}^{(c)}(\mathbf{x}, t_0 + \tfrac{1}{2}) = [\mathbf{x} - \mathbf{X}(t_0)] \times \mathbf{F}^{(c)}(\mathbf{x}, t_0 + \tfrac{1}{2}), \tag{11}$$

where $\mathbf{U}'$ is the local velocity of the solid particle and $\mathbf{X}(t_0)$ is the position vector of the center of mass. The force and torque are assumed to be distributed through the time interval $[t_0, t_0+1]$. When a virtual fluid node is uncovered due to the motion of a solid particle, the transferred force and torque are given, respectively, by

$$\mathbf{F}^{(c)}(\mathbf{x}, t_0+\tfrac{1}{2}) = -\rho(\mathbf{x}, t_0)[\mathbf{u}(\mathbf{x}, t_0)-\mathbf{U}']$$

and

$$\mathbf{T}^{(c)}(\mathbf{x}, t_0+\tfrac{1}{2}) = [\mathbf{x}-\mathbf{X}(t_0)]\times\mathbf{F}^{(c)}(\mathbf{x}, t_0+\tfrac{1}{2}).$$

It is important to note that these rules are Galilean invariant.

As the solid particles move, the total number of fluid nodes containing fluid mass can slightly fluctuate. This fluctuation is insignificant in the macroscopic level.

## 2.4. Solid-Fluid Boundary Condition

The simplest scheme to calculate the momentum transfer between fluid and solid particle is the "link-bounce-back" boundary condition, where the boundary is always assumed to be located at the middle of the boundary links. Although more accurate boundary conditions can be implemented by combining the "link-bounce-back" scheme with spatial interpolation of first or second order[17] or by introducing a continuous parameter for the fluid volume in each cell,[18] the simplest boundary condition is considered here for the purpose of presenting the ALD' method. The higher order boundary rules can be easily implemented with this method.

For a stationary solid surface, the probability distribution function at $t+1$ is given by

$$f_{\sigma i}(\mathbf{x}, t+1) = \mathsf{P}_{\mathrm{n-s}}(\mathbf{0}) f_{\sigma i}(\mathbf{x}, t_+) \equiv \begin{cases} f_{\sigma i'}(\mathbf{x}, t_+), & \text{if } (\sigma i') \text{ is BL,} \\ f_{\sigma i}(\mathbf{x}+\mathbf{e}_{\sigma i'}, t_+), & \text{otherwise,} \end{cases} \tag{12}$$

where $\mathsf{P}_{\mathrm{n-s}}(\mathbf{0})$ is the no-slip propagator for a stationary wall and BL refers to the boundary link, that is, the link that connects the physical fluid node to the virtual fluid node. The distribution function at the no-slip stationary boundary node is given by

$$f_{\sigma i}(\mathbf{x}, t+1) = \mathsf{P}_{\mathrm{n-s}}(\mathbf{0})\, \mathsf{C} f_{\sigma i}(\mathbf{x}, t). \tag{13}$$

For a moving solid surface, however, the distribution function is given by

$$f_{\sigma i}(\mathbf{x}, t+1) = \mathsf{P}_{\mathrm{n-s}}(\mathbf{u}_{\mathrm{b}})\, f_{\sigma i}(\mathbf{x}, t_+) \equiv \begin{cases} f_{\sigma i'}(\mathbf{x}, t_+) + 2\rho B_\sigma \mathbf{u}_b \cdot \mathbf{e}_{\sigma i}, & \text{if } (\sigma i') \text{ is BL,} \\ f_{\sigma i}(\mathbf{x}+\mathbf{e}_{\sigma i'}, t_+), & \text{otherwise.} \end{cases} \tag{14}$$

where $\mathbf{u}_b$ is the velocity of the solid object at the midpoint of the boundary link and $\rho$ is the density at node $\mathbf{x}$. In this paper, the value of $\rho$ at time $t$ is used in Eq. (14). One can also use $\rho$ at time $t+1$ without any significant change in the result.

During collision, the momentum transferred to the solid particle is given by

$$\delta \mathbf{p}_{\sigma i} = 2\mathbf{e}_{\sigma i'}[f_{\sigma i}(\mathbf{x}, t+1) - \rho B_\sigma \mathbf{u}_b \mathbf{e}_{\sigma i}]$$

if the fluid node is a physical one. If the node interacting with the solid object is a virtual fluid node inside the solid object, the solid object will not gain any momentum during collision, and therefore, $\delta \mathbf{p}_{\sigma i} = 0$.

## 2.5. Virtual Nodes when Two Particles Are Near Contact

When the separation between two suspended solid particles becomes smaller than a unit lattice dimension, two different situations, as shown in Fig. 1, are possible. In case (a) of Fig. 1, which is an "exceptional" case (nongeneric), at least one layer of fluid nodes always exists in the gap as the two particles approach each other. However, this case rarely occurs in the simulations. In most cases, there is no fluid node in the gap when the particle separation is smaller than the lattice size, that is, case (b). In this case,

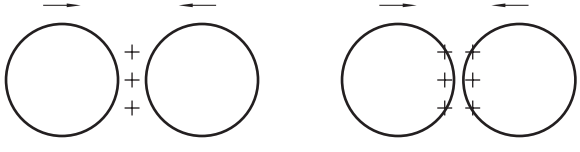

(a) At least one layer of fluid nodes in the gap

(b) No fluid nodes in the gap

Fig. 1. When the separation between two particles is less than a lattice unit, the minimum gap may contain (a) one layer of fluid nodes or (b) no fluid nodes. Results with these two lattice arrangements, referred to as cases (a) and (b), are presented in some of the following figures.

the operator defined in Eq. (14) is not applicable, and the rule for calculating the distribution function $f_{\sigma i}(\mathbf{x}, t+1)$ must be modified because the two nodes on the separation link are now covered by the solid particles and no longer contain real fluid. In ALD' method, both nodes become virtual nodes.

To explain this case in more detail, let's assume that there are two solid particles, say, $I$ and $J$, as shown in Fig. 2. The initial point of link $\mathbf{e}_{\sigma i}$ is node $\mathbf{x}$, just inside the solid boundary of particle $I$, while the final point of link $\mathbf{e}_{\sigma i}$ is node $\mathbf{y}$, just inside the solid boundary of particle $J$. The rule for calculating the interaction between the virtual node at the solid surface and its neighboring fluid nodes must be modified. Both nodes $\mathbf{x}$ and $\mathbf{y}$ are considered to be physical fluid nodes. When the interaction between node $\mathbf{x}$ and particle $I$ is being considered, the distribution function at node $\mathbf{x}$ at time $t+1$ on link $\mathbf{e}_{\sigma i}$ is given by

$$f_{\sigma i}(\mathbf{x}, t+1) = \mathsf{P}_{\mathrm{n-s}}(\mathbf{u}_{\mathrm{b}})\, f_{\sigma i}(\mathbf{x}, t_+) = f_{\sigma i'}(\mathbf{x}, t_+) + 2\rho B_\sigma \mathbf{u}_b \cdot \mathbf{e}_{\sigma i}, \qquad (15)$$

and $\mathbf{u}_b$ is the velocity of solid particle $I$ at $\mathbf{x}+\frac{1}{2}\mathbf{e}_{\sigma i}$. Consequently, the momentum transfer to solid particle $I$ is given by

$$\delta \mathbf{p}_{\sigma i} = 2\mathbf{e}_{\sigma i'}[f_{\sigma i}(\mathbf{x}, t+1) - \rho B_\sigma \mathbf{u}_b \mathbf{e}_{\sigma i}].$$

The same rule is used to calculate the interaction between node $\mathbf{y}$ and particle $J$.

Since node $\mathbf{y}$ is considered as a fluid node, as if it was moved outside particle $J$, node $\mathbf{y}'$ should be considered as a boundary node, with distribution function in direction $\mathbf{e}_{\sigma i}$ updated by

$$f_{\sigma i}(\mathbf{y}', t+1) = \mathsf{P}_{\mathrm{n-s}}(\mathbf{u}'_{\mathrm{b}})\, f_{\sigma i}(\mathbf{y}', t_+) = f_{\sigma i'}(\mathbf{y}', t_+) + 2\rho B_\sigma \mathbf{u}'_b \cdot \mathbf{e}_{\sigma i}.$$

There is no momentum transformed in this collision. The same rule is used to update the distribution function at node $\mathbf{x}'$.

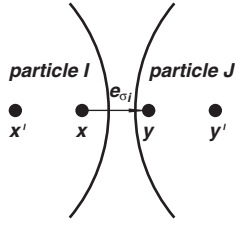


Fig. 2. Notation used in the calculation of the interaction between two solid particles near contact. $\mathbf{x}'$, $\mathbf{x}$, $\mathbf{y}$, and $\mathbf{y}'$ are virtual fluid nodes. Node $\mathbf{x}$ ($\mathbf{y}$) are considered as fluid nodes in calculation of the interaction between particle $I$ ($J$) and fluid in the gap area.

For case (a) in Fig. 1, there is at least one layer of fluid nodes in the gap. The virtual boundary nodes in the solid particles are also considered as fluid nodes, and the same rules for case (b) are used to update the distribution function and to calculate the momentum transfer.

When a solid particle is very close to a solid wall, the interaction between the wall and the particle is treated in a similar manner.

With the momentum transferred to the solid particle through each link, the impulse force exerted on the particle is given by

$$\mathbf{F}_{\sigma i}^{(b)}(\mathbf{x}, t_0+\tfrac{1}{2}) = \delta \mathbf{p}_{\sigma i} / \Delta t. \tag{16}$$

And the torque with respect to the center of mass, $\mathbf{X}$, is given by

$$\mathbf{T}_{\sigma i}^{(b)}(\mathbf{x}, t_0+\tfrac{1}{2}) = [\mathbf{x}-\mathbf{X}(t_0)] \times \mathbf{F}_{\sigma i}^{(b)}(\mathbf{x}, t_0+\tfrac{1}{2}). \tag{17}$$

## 2.6. Lubrication Forces Included in the ALD′ Method

In many particulate flow problems, the lubrication forces between two particles significantly influence the bulk flow behavior. The numerical procedure outlined above cannot accurately capture the force separating two particles when the particle separation becomes much smaller than the lattice dimension. To further resolve the forces separating the two particles about to collide, one can use the results from linearized lubrication approximation and include the force in analytical form. The procedure used in the ALD′ method to capture the singular lubrication forces when the gap, $\epsilon$, between two solid surfaces tends to zero is outlined in the following paragraphs. Note, however, that in direct simulation of particle collision a minimum gap, comparable to the solid surface roughness, should be included in the model to capture actual particle collision, as it occurs with real particles.

In this model, the lubrication forces are included using links connecting two virtual boundary nodes from two surfaces near contact (Fig. 2), defined as "bridge" links. In the case presented by Fig. 1(a), a link between a virtual boundary node and the adjacent fluid node is referred to as a "half-bridge" link. A "pair of half-bridge" links refers to two half-bridge links along a straight line that share a single fluid node between them.

The idea here is to determine an element of force, $df$, for each bridge link and each pair of half-bridge links which accurately account for the lubrication force. This element of force applies on the linked surface elements. The direction of the element of force should be along the bridge link or the pair of half-bridge links, while its magnitude should be such that the

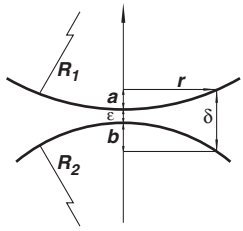


Fig. 3. Notations used in calculating the lubrication force between two surface elements.

summation over every bridge link and every pair of half-bridge links provides the correct lubrication force.

Let's consider the element of force, $df'$, given by

$$df' = \frac{3}{2}\frac{\nu\rho U}{\lambda\delta^2}, \tag{18}$$

where $\delta = \delta(r)$ is the surface separation, as defined in Fig. 3, and $\lambda$ depends on the surface curvature. In the following paragraphs, we will first demonstrate that this relation provides results in agreement with analytical results for two spheres based on linearized lubrication theory when two surface elements are joined by a single off-diagonal link along the direction parallel to the centerline. We will then generalize this relation to cases where more than one link may exist between surface elements.

If the two particles are spheres, the surface curvature, $\lambda$, is given by

$$\lambda = \frac{1}{2}\left(\frac{1}{R_1} + \frac{1}{R_2}\right),$$

where $R_1$ and $R_2$ are the radii of curvature of the two surface elements. The summation of the elements of force over every surface element, given by

$$F = \sum df' = \int \frac{3}{2}\frac{\nu\rho U}{\lambda\delta^2}\, d\sigma, \tag{19}$$

provides the correct lubrication force between two spheres ($d\sigma$ represents an infinitesimal surface element). From simple geometric considerations, if $R_1 \gg a$

$$r^2 = (2R_1 - a)\, a \simeq 2R_1 a, \tag{20}$$

and if $R_2 \gg b$

$$r^2 = (2R_2 - b)\, b \simeq 2R_2 b, \tag{21}$$

hence

$$\delta = \epsilon + a + b = \epsilon + r^2\lambda. \tag{22}$$

Then

$$d\sigma = 2\pi r\, dr = \frac{\pi}{\lambda}\, d\delta, \tag{23}$$

and subsequently, the summation (19) becomes

$$F = -\frac{3\pi}{2\lambda^2}\frac{\nu\rho U}{\epsilon} \tag{24}$$

which is the same as the relation given by Cox (1974) for two spheres.

As mentioned above, Eq. (18) only applies to cases where the two surface elements are connected by a single off-diagonal link. Considering that the lubrication force becomes important when the separation between two particles is much less than the lattice dimension, the general formulation should apply to cases where more than one bridge link exists between two surface elements. Therefore, the element of force, $df'$, must be modified by a weighing factor, $q$, to include the effect of multiple links. The general form of the element of force, $df$, is therefore given by

$$df = q\, df' = \frac{3}{2}\frac{\nu\rho U}{\lambda\delta^2}\, q, \tag{25}$$

where the weighing factor $q$ depends on the number and configuration of the bridge and half-bridge links. One can use an averaged weighing factor defined by

$$\bar{q} = \frac{\sum q\, df'}{\sum df'}.$$

In our simulation we have found that the value of $\bar{q} \simeq 0.6$.

The force element, $df$, along the direction of a bridge link or a pair of half-bridge links, has a significant contribution to the lubrication force only when $\delta$ is very small. If the value of $\delta$ is larger than the length of the link, the contribution of the "lubrication" component, $df$, will be insignificant.

Also, since a link can be in diagonal or off-diagonal directions, it is necessary to keep the results isotropic and independent of the lattice structure. Therefore, the elements of lubrication force along diagonal links ($\sigma = 2$) should be scaled as one-half of the force along off-diagonal links ($\sigma = 1$). This is consistent with the equilibrium distribution function (9), where the coefficients of group 2 in the diagonal direction are one-half of the corresponding coefficients of group 1 in the off-diagonal direction. With the above derivation, the element of lubrication force, in general form, is given by

$$df = \begin{cases} \dfrac{3\bar{q}}{2c_\sigma^2 \lambda} \nu \rho U \left( \dfrac{1}{\delta^2} - \dfrac{1}{c_\sigma^2} \right), & \text{if} \quad \delta < c_\sigma \\ 0, & \text{if} \quad \delta \geqslant c_\sigma. \end{cases} \tag{26}$$

The force and the torque on the solid particle along this link ($\sigma i$), $\mathbf{F}^{(d)}$ and $\mathbf{T}^{(d)}$, are given by

$$\mathbf{F}^{(d)}(\mathbf{x}, t) = df \frac{\mathbf{e}_{\sigma i}}{c_\sigma},$$

and

$$\mathbf{T}^{(d)}(\mathbf{x}, t) = [\mathbf{x} - \mathbf{X}(t)] \times \mathbf{F}^{(d)}(\mathbf{x}, t),$$

respectively. The total lubrication force and its torque on a solid particle is then given by

$$\mathbf{F}^{\text{lub}}(t) = \sum_{BS} \mathbf{F}^{(d)}(\mathbf{x}, t)$$

and

$$\mathbf{T}^{\text{lub}}(t) = \sum_{BS} \mathbf{T}^{(d)}(\mathbf{x}, t),$$

respectively, where BS stands for the bridge links and pair of half-bridge links. Simulation results show that with $df$ from Eq. (26) the summation over two spherical surfaces is in agreement with theoretical prediction. In general, this expression applies to smooth surfaces where the spatial variation of local curvatures is not very large.

Accordingly, the force element, $df$, for two-dimensional cases, is given by

$$df = \begin{cases} \dfrac{3}{c_\sigma^4 \sqrt{\lambda}} \nu \rho U \left( \dfrac{1}{\delta^{3/2}} - \dfrac{1}{c_\sigma^{3/2}} \right), & \text{if} \quad \delta < c_\sigma \\ 0, & \text{if} \quad \delta \geqslant c_\sigma. \end{cases} \tag{27}$$

In the following sections the accuracy and validity of the method outlined above will be presented.

## 2.7. Equations Governing the Motion of a Solid Particle Suspended in Fluid

The total force and torque on the solid particle during $[t_0, t_0+1]$, except for the lubrication force, are given by

$$\mathbf{F}(t_0+\tfrac{1}{2}) = \sum_{BN} \sum_{\sigma i} \mathbf{F}_{\sigma i}^{(b)}(\mathbf{x}+\tfrac{1}{2}\,\mathbf{e}_{\sigma i'}, t_0+\tfrac{1}{2}) + \sum_{CN} \mathbf{F}^{(c)}(\mathbf{x}, t_0+\tfrac{1}{2}) \tag{28}$$

and

$$\mathbf{T}(t_0+\tfrac{1}{2}) = \sum_{BN} \sum_{\sigma i} \mathbf{T}_{\sigma i}^{(b)}(\mathbf{x}+\tfrac{1}{2}\,\mathbf{e}_{\sigma i'}, t_0+\tfrac{1}{2}) + \sum_{CN} \mathbf{T}^{(c)}(\mathbf{x}, t_0+\tfrac{1}{2}), \tag{29}$$

respectively, where BN stands for the boundary nodes and CN for covered and uncovered nodes due to the motion of the particle.

The total force and torque, excluding the lubrication force, at time $t_0$, averaged over time interval $[t_0-1, t_0+1]$, are given by

$$\mathbf{F}(t_0) = \tfrac{1}{2}[\mathbf{F}(t_0+\tfrac{1}{2}) + \mathbf{F}(t_0-\tfrac{1}{2})] \tag{30}$$

and

$$\mathbf{T}(t_0) = \tfrac{1}{2}[\mathbf{T}(t_0+\tfrac{1}{2}) + \mathbf{T}(t_0-\tfrac{1}{2})]. \tag{31}$$

With the net force and torque from the above equations, the motion of the solid particle from $t = t_0$ through $t = t_0+1$ is determined by solving Newton's equations given by

$$M \frac{d\mathbf{U}(t)}{dt} = \mathbf{F}(t_0) + \mathbf{F}^{\text{lub}}(t), \tag{32}$$

for translation, and

$$\mathbf{I}\cdot\frac{d\boldsymbol{\Omega}(t)}{dt}+\boldsymbol{\Omega}(t)\times[\mathbf{I}\cdot\boldsymbol{\Omega}(t)]=\mathbf{T}(t_0)+\mathbf{T}^{\text{lub}}(t), \tag{33}$$

for rotation of the solid particle. Here $M$ is the mass of the suspended particle, $\mathbf{I}$ is the inertial tensor, and $\Omega$ is the angular velocity. In this simulation, these equations are solved using a fourth-order accurate Runge–Kutta integration procedure to obtain the complete motion of the suspended solid particles in the fluid. Note that the variation of the lubrication component of force and torque per lattice time unit increases as the surface separation decreases. In order to accurately resolve the lubrication force, the lattice time unit is divided accordingly into substeps in the integration procedure.

## 3. PARAMETERS IN THE LATTICE-BOLTZMANN EQUATION

The purpose of this section is to demonstrate that there is no adjustable parameter in the lattice-Boltzmann method. There are three numerical parameters, $\tau$, $\Delta x$, and $\Delta t$, in the lattice-Boltzmann equation (1), where $\Delta x$ and $\Delta t$ are the length of the lattice unit and the magnitude of the time step, respectively. As in any simulation, $\Delta x$ and $\Delta t$ must be sufficiently smaller than the characteristic length scale and the characteristic time scale of the system. Since the surface of the particle is projected on a discrete computation lattice, the boundary is always assumed to be at the midpoint of the boundary nodes when the interaction between solid particle and fluid is considered.[1, 2, 6] When the size of the solid particle relative to $\Delta x$ increases, the surface is defined more precisely. The lattice-Boltzmann method is accurate only when the grid is very fine, or, in other words, the particle surface is projected onto a large number of lattice nodes.

The flow problem should be defined by the nondimensional parameters. For example, problems concerned with incompressible flow past blunt bodies are defined based on the Reynolds number, $Re = ud/\nu$, where $u$ is the free stream velocity scale, $d$ is the characteristic length of the blunt body, and $\nu$ is the kinematic viscosity. For particles in shear flow, the defining parameter is the particle Reynolds number based on the rate of shear, $\dot{\gamma}$, that is $Re = \dot{\gamma}d^2/\nu$. When gravity, $g$, is considered, then the Froude number, defined as $Fr = u^2/gd$, becomes the second parameter in the problem.

As the first example, consider the flow over a blunt body. In this example, the physical variables, fluid properties and nondimensional parameters based on the physical quantities, are defined by subscript, $s$,

where the variable in lattice scale has no subscript. Then $U_s$ and $d_s$ are the characteristic velocity and length, respectively; and $v_s$ is the kinematic viscosity. Reynolds number is defined as $Re_s = U_s d_s / v_s$. The Reynolds number based on the corresponding parameters in the lattice scale is defined as $Re = Ud/v$. The parameters $u$, $d$, and $v$ in the lattice scale should be set such that $Re_s = Re$. Therefore, $U_s d_s / v_s = Ud/v$, or

$$v = v_s \left(\frac{U}{U_s}\right)\left(\frac{d}{d_s}\right),$$

where

$$d = d_s / \Delta x,$$

and

$$U = U_s(\Delta t / \Delta x).$$

Since the Mach number has to be small for incompressible flow, the characteristic lattice velocity scale, $U$, is usually set at about 0.1 or less with corresponding Mach number less than $(0.1/\sqrt{1/3} =)\ 0.173$. For a problem where $Re = 10$, for example, then $d/v = 100$; and if the characteristic length, for example the diameter of the particle, is discretized by 20 lattice units, then $d = 20$ and $v = 0.2$. The parameter that needs to be specified in the lattice-Boltzmann equation (i.e., Eq. (1)) is the relaxation time constant $\tau = (6v+1)/2$. Therefore, in this example, $\tau = 2.2/2 = 1.1$.

As a second example, closer to the cases considered in the next section, consider a circular cylinder moving with a translational velocity $u_s = 0.0024$ cm/sec in a channel filled with fluid. The radius of the cylinder is $R_s = 1.2$ cm. The fluid density is $\rho_s = 1\ \mathrm{g/cm^3}$, and viscosity is $v_s = 0.01\ \mathrm{cm^2/sec}$. The width of the channel is $L_s = 4R_s$, and the length is $2L_s$. No-slip boundary condition is used for the channel walls, and periodic boundary condition is used for the inlet and outlet. Reynolds number in this case is $Re_s = u_s(2R_s)/v_s = 0.576$. The Reynolds number based on the lattice-Boltzmann computational parameters is given by

$$Re = u(2R)/v.$$

As long as $Re = Re_s$, the lattice-Boltzmann simulation will accurately compute the flow field and the particle dynamics. If $\Delta x = 0.1$ cm is chosen, the radius of the cylinder is $R = 12$. When $v = 1/6$ (i.e., $\tau = 1$), the time increment, $\Delta t$, is 1/6 sec. The velocity, $u$, of the cylinder is 0.004, much smaller than the speed of sound in the lattice-Boltzmann scale (i.e.,

$c_s = \sqrt{1/3}$). Lattice-Boltzmann simulation results show that the drag coefficient,

$$f = F_s/u_s v_s \rho_s = F/uv\rho = 12.4.$$

Hence, the force on the cylinder is

$$F_s = f u_s v_s \rho_s = 2.98 \times 10^{-4} \text{ dyn/cm}.$$

Different values of $\Delta x$ and $v$ have been chosen in this simulation. Results are summarized in Fig. 4(a). Larger value of $R$ means smaller value of $\Delta x$. When $R$ is sufficiently large, different values of $v$ result in the same drag coefficient, denoted by $f^*$. On the other hand, if $R < 8$ in this example, $\Delta x$ is too large, and the simulation results may apparently deviate from $f^*$. This is expected because, like any other numerical method, there must be sufficient number of lattice nodes upon which the projected flow field can be well resolved, and consequently the results become independent of the relaxation parameter.

As an example of a three-dimensional case, a sphere moving with a constant speed in a channel filled with fluid is considered. The simulation results, summarized in Fig. 4(b), show that the drag coefficient is independent of the different choices of $v$ when the radius, $R$, of the sphere is sufficiently large. These examples clearly demonstrate that there is no adjustable parameter in the lattice-Boltzmann method. To obtain reliable results in the simulation, the increments $\Delta x$ and $\Delta t$ must be sufficiently small—similar to any other computational method.

## 4. HYDRODYNAMIC INTERACTIONS

To evaluate the accuracy and effectiveness of the current computational method, the hydrodynamic interactions between two solid objects in relative motion and in close contact are discussed in this section.

Four different cases are being considered in this section. Two spheres approaching each other and a sphere approaching a flat wall are the three-dimensional simulations. For two-dimensional cases, two circular cylinders approaching each other and a circular cylinder approaching a flat wall are considered.

### 4.1. Two Spheres in a Three-Dimensional Channel

In this section we consider two spheres in a three-dimensional channel approaching each other with a constant velocity.

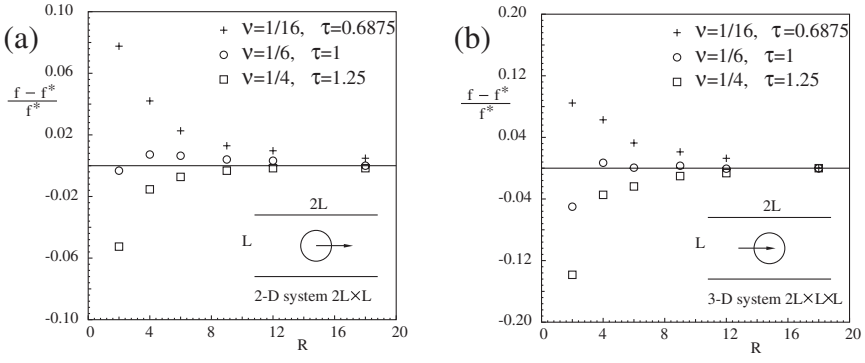


Fig. 4. The drag force on a moving particle in a channel filled with fluid. (a) A circular cylinder of radius $R$ in a two-dimensional channel $2L$ long and $L$ wide, where $L = 4R$. $f^*$, the drag coefficient for $R = 48$, is independent of $\tau$. (b) A sphere of radius $R$ in a three-dimensional channel $2L \times L \times L$, where $L = 4R$. $f^*$, the drag coefficient for $R = 18$, showing that the results are independent of $\tau$.

The radius of the spheres are $R_1$ and $R_2$, and the center-to-center distance between the two spheres is $d$. The separation value, $s$, between the two spheres is given by

$$s = \epsilon\lambda,$$

where

$$\epsilon = d - R_1 - R_2,$$

and

$$\lambda = \frac{1}{2}\left(\frac{1}{R_1} + \frac{1}{R_2}\right).$$

For two identical spheres, where $R = R_1 = R_2$,

$$\lambda = \frac{1}{R}, \qquad \text{and} \qquad s = \frac{d}{R} - 2.$$

The leading order force, $f$, based on lubrication approximation between these two spheres in three-dimensional space is given by refs. 19 and 20:

$$\frac{f}{2\rho\nu U/\lambda} = \frac{3\pi}{4s} + C_w, \tag{34}$$

where $\rho$ and $\nu$ are the fluid density and viscosity, respectively, $U$ is the relative velocity of two particles, and $C_w$ is a constant depending on the wall effect. If the channel is infinitely large, then $C_w = 0$.

The computations are based on the ALD' method outlined above. The flow field and the lubrication force between two spheres moving toward each other with a constant speed are computed in a rectangular channel. The size of the rectangular channel is $64 \times 32 \times 32$, and the radius of the spheres are $R = 4.25$. With four different sets of values for $\nu$ and $U$, the lubrication force at Reynolds number $Re = 0.57$ is computed and results are presented in Fig. 5. The lubrication force from Eq. (34) is also plotted as a solid line in the same figure for comparison. The $x$-axis, expressing the width of the gap between two spheres, is scaled by $\lambda = 1/R$. The gap in the unit of lattice spacing is also shown at the upper edge of the figure. It is clear that the improved ALD' method, presented above, significantly extends the range of application and the accuracy for near contact particles.

The simulation results are relatively in good agreement with the theoretical prediction when $\epsilon \geqslant 1$. Furthermore, the general divergence behavior of the lubrication forces near contact is reproduced for particle separations of as small as 0.1 lattice spacing and beyond. Notice that in simulations of multiparticle systems, there is usually no fluid node on the line of their centers when two particles are almost in contact; therefore, case (b) of Fig. 1 is more probable than case (a). Considering that the ALD method fails to apply when $\epsilon \leqslant 2$, it is clear that the improved ALD' method, presented above, significantly extends the range of application and the accuracy for near contact particles.

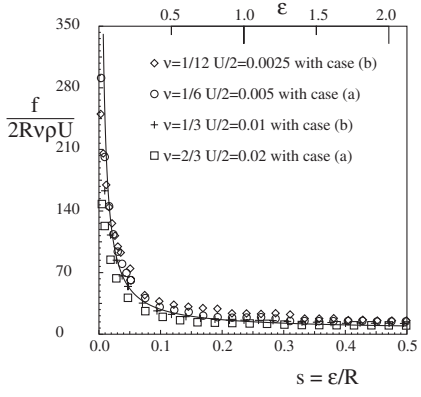


Fig. 5. Normal force in interaction between two identical spheres with radius $R = 4.25$ near contact. The system size is $64 \times 32 \times 32$. The solid line is obtained from lubrication theory.

## 4.2. A Sphere Approaching a Flat Wall

Significant interaction between particles and flat boundaries occurs in confined channels. To examine the accuracy of the ALD' method for this case, in this section the ALD' method is applied to a sphere approaching a flat wall.

In this simulation the particle is moving toward a flat wall with a constant velocity, $U = 0.02$. Keeping Reynolds number fixed at $Re = 1.044$, three cases with values of radius and viscosity given by $(R, \nu) = (3.2625, 1/8)$, $(4.35, 1/6)$, and $(6.525, 1/4)$, are considered. The results show very good agreement with theoretical prediction Eq. (34), presented in Fig. 6 as a solid line.

The requirement for the minimum separation between two solid surfaces, either particles or particle and a wall, has been considerably reduced with the ALD' method. In the case considered here, the normalized force is accurately calculated for the particle almost in contact with the wall even up to normalized force at 400 where the separation distance is much smaller than a single lattice unit.

## 4.3. Two Circular Cylinders in a Two-Dimensional Channel

Results of the two-dimensional simulations for circular cylinders approaching each other corresponding to cases (a) and (b) of Fig. 1 are presented in Figs. 7 and 8, respectively. The computational domain is $2L \times L$, and the radius of the circular cylinder is $0.2875L$. The two particles

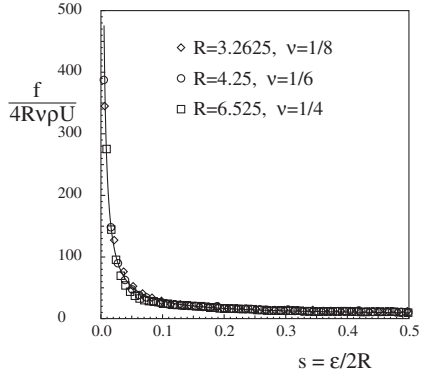


Fig. 6. Normal force on a sphere approaching a flat wall with constant velocity $U = 0.02$. The solid line is obtained through classical lubrication theory. Reynolds number here is $Re = 1.044$.

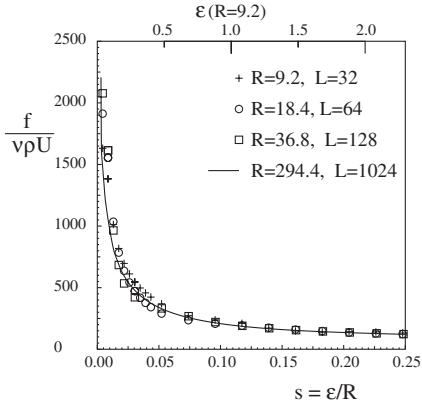


Fig. 7. Normal force between two identical circular cylinders in 2-D domain, approaching each other with speeds $\pm U/2 = \pm 0.01$, respectively. There is always at least one layer of fluid nodes between the two particles. The system size is $2L \times L$, and the radius of the cylinders is $R = 0.2875L$. The gap in the unit of lattice spacing when $R = 9.2$ is also shown at the upper edge of the figure. Note the difference in definition of the nondimensional force between the two-dimensional case, presented in this and following two figures, compared to the three-dimensional case presented in Fig. 5 and 6.

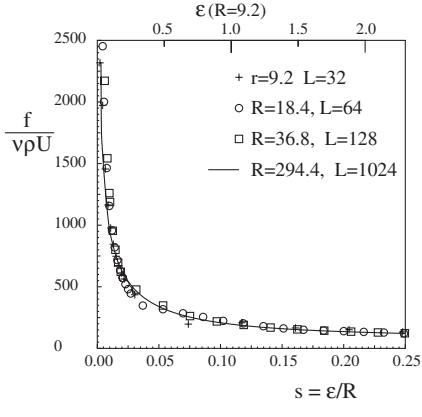


Fig. 8. Normal force between two identical circular cylinders in 2-D domain, approaching each other with speeds $\pm U/2 = \pm 0.01$, respectively. No fluid nodes between the solid particles when they are very close to each other. The system size is $2L \times L$, and the radius of the cylinders is $R = 0.2875L$. The gap in the unit of lattice spacing when $R = 9.2$ is also shown at the upper edge of the figure.

are approaching each other with constant velocities $\pm U/2 = \pm 0.01$, respectively. With $L = 32$ and $\nu = 1/8$, the simulation has already provided reliable results for the particle separation as small as $\epsilon \simeq 0.1$.

The accuracy of the simulation is examined by comparing with a "double-size calculation," in which both $\Delta x$ and $\Delta t$ are reduced by a factor 2, while both Mach number and Reynolds number are kept unchanged, and consequently, the value of viscosity, $\nu$, is doubled. A series of successive double-size calculations are carried out up to $L = 1024$. The simulation results for various grid sizes of $L = 32$ as well as $L = 64$ and 128 are compared with the very fine grid size of $L = 1024$ lattice units. This comparison demonstrates the advantage of the present method where a relatively coarse grid of 32 to 128 cells provides results that are nearly as accurate as the very fine grid size of 1024 lattice units.

### 4.4. A Circular Cylinder and a Flat Wall

Results for the lubrication force between a circular cylinder and a flat wall in a two-dimensional space are shown in Fig. 9. The system size is $L \times L$ with $L = 64$ and 128, respectively. A circular cylinder with radius $R = 0.14357L$ is moving toward the flat wall with constant velocity $U = 0.01$. With the smallest system, $L = 64$, the viscosity is $\nu = 1/8$. The other three larger systems are designed for a series of successive "double-size" calculations. The results obtained by simulation with smaller systems show nearly perfect agreement with the finest lattice, that is $L = 1024$, presented with a solid line in Fig. 9.

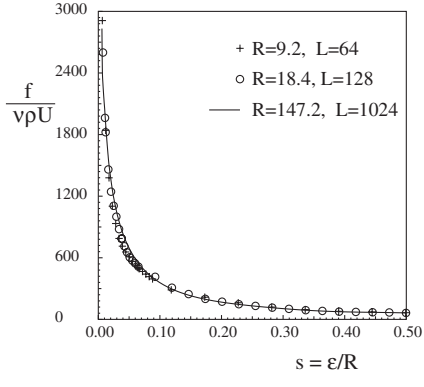


Fig. 9. Normal force on a circular cylinder approaching a flat wall with constant velocity $U = 0.01$. The solid line is calculated with a very fine lattice ($R = 147.2$, $L \times L = 1024 \times 1024$), which is assumed to provide accurate lubrication force when $s \geqslant 0.01$. The results with coarser lattice are shown by $+$: $R = 9.2$, $L \times L = 64 \times 64$ and $\bigcirc$: $R = 18.4$, $L \times L = 128 \times 128$, respectively.

## 5. CONCLUDING REMARKS

The purpose of the present work is to extend the ALD method to simulation of suspended particles near contact, without the requirement of having two or more lattice nodes in between the solid particles. Considering the significant importance of the lubrication force in the dynamics of suspended particles in fluid, the necessity of the extension of the ALD method is obvious. The ALD' method, described in Section 2, is able to correctly calculate the interaction between solid objects near contact. The accuracy of the simulation when two surfaces are near contact is greatly improved eventhough the computational domain consists of fewer lattice nodes.

In order to get more satisfactory simulation results, the following ways of modification of this method may be considered. The collision operator can be replaced by a generalized one provided by Lallemand and Luo.[21] This may provide a more flexible model and in some cases may provide more accurate and stable results. Our method can be simply extended by adding higher-order boundary rules.[17, 18] The model provided by Heelmels *et al.*[22] is a modified Shell model where it accurately conserves mass and momentum.

## ACKNOWLEDGMENTS

This work has been supported in part by the National Science Foundation through Grant CTS-0130326.

## REFERENCES

1. A. J. C. Ladd, Numerical simulations of particulate suspensions via a discretized Boltzmann equation, Part 1, Theoretical foundation, *J. Fluid Mech.* **271**:285 (1994).
2. A. J. C. Ladd, Numerical simulations of particulate suspensions via a discretized Boltzmann equation, Part 2, Numerical results, *J. Fluid Mech.* **271**:311 (1994).
3. C. K. Aidun and Y. Lu, Lattice-Boltzmann simulation of solid particles suspended in fluid, *J. Stat. Phys.* **81**:49 (1995).
4. C. K. Aidun, Y. Lu, and E. Ding, Dynamic simulation of particles suspended in fluid, The 1997 ASME Fluids Engineering Division Summer Meeting, (FEDSM'97), June 22–26 (1997).
5. D. L. Koch and A. J. C. Ladd, Moderate Reynolds number flows through periodic and random arrays of aligned cylinders, *J. Fluid Mech.* **349**:31 (1997).
6. C. K. Aidun, Y. Lu, and E. Ding, Direct analysis of particulate suspensions with inertia using the discrete Boltzmann equation, *J. Fluid Mech.* **373**:287 (1998).
7. C. K. Aidun and D. Qi, A new method for analysis of the fluid interaction with a deformable membrane, *J. Stat. Phys.* **90**:145 (1998).
8. D. Qi, Lattice Boltzmann simulations of particle in no-zero-Reynolds-number flows, *J. Fluid Mech.* **385**:41 (1999).

9. E. Ding and C. K. Aidun, The dynamics and scaling law for particles suspended in shear flow with inertia, *J. Fluid Mech.* **423**:317 (2000).
10. A. J. C. Ladd, Hydrodynamic screening in sedimenting suspensions of non-Brownian spheres, *Phys. Rev. Lett.* **76**:1392 (1996).
11. A. J. C. Ladd, Sedimentation of homogeneous suspensions of non-Brownian spheres, *Phys. Fluids* **9**:491 (1997).
12. G. R. McNamara and G. Zanetti, Use of the Boltzmann equation to simulate lattice-gas automata, *Phys. Rev. Lett.* **61**:2332 (1988).
13. H. Chen, S. Chen, and W. H. Matthaeus, Recovery of the Navier–Stokes equations using a lattice-gas Boltzmann method, *Phys. Rev. A* **45**:R5339 (1992).
14. S. Hou, Q. Zou, S. Chen, G. Doolen, and A. C. Cogley, Simulation of cavity flow by lattice-Boltzmann method, *J. Comput. Phys.* **118**:329 (1995).
15. L. Luo, Unified theory of the lattice Boltzmann models for nonideal gases, *Phys. Rev. Lett.* **81**:1618 (1998).
16. X. He and L. Luo, Theory of the lattice Boltzmann method: From the Boltzmann equation to the lattice Boltzmann equation, *Phys. Rev. E* **56**:6811 (1997).
17. M. Bouzidi, M. Firdaouss, and P. Lallemand, Momentum transfer of a Boltzmann-lattice fluid with boundaries, *Phys. Fluids* **13**:3452 (2001).
18. R. Verberg and A. J. C. Ladd, Lattice-Boltzmann model with sub-grid-scale boundary conditions, *Phys. Rev. Lett.* **84**:2148 (2000).
19. R. G. Cox, The motion of suspended particles almost in contact, *Int J. Multiphas. Flow* **1**:343 (1974).
20. I. L. Claeys and J. F. Brady, Lubrication singularities of the grand resistance tensor for two arbitrary particles, *Physicochem. Hydrodyn.* **11**:261 (1989).
21. P. Lallemand and L. Luo, Theory of the lattice Boltzmann method: Dispersion, dissipation, isotropy, Galilean invariance, and stability, *Phys. Rev. E* **61**:6546 (2000).
22. M. W. Heemels, M. H. J. Hagen, and C.P. Lowe, Simulating solid colloidal particles using the lattice-Boltzmann method, *J. Comput. Phys.* **164**:48 (2000).